# CASLE 2017

**Sustainable Development Goals: a time for innovations and investment in land administration and management**

## 10 - 11th August 2017
## Dar es Salaam – Tanzania

**Editors**
Dr Patrick Manu
Mr Tony Westcott
Professor Dr Alan Spedding

# EFFECT OF CAMERA CALIBRATION ON THE ACCURATE GENERATION OF DIGITAL ELEVATION MODELS FROM UAV ACQUIRED LOW PERCENTAGE OVERLAPPING IMAGES

Oluibukun Gbenga Ajayi[1], Ifeanyi Jonathan Nwadialor[2], Ifeanyi Chukwudi Onuigbo[3], and Olurotimi Adebowale Kemiki[4].
[1], [2], [3] *Department of Surveying and Geoinformatics, Federal University of Technology, Minna, Nigeria.*
[4]*Department of Estate Management, Federal University of Technology, Minna, Nigeria.*

Using low percentage overlapping images (15-20% sidelap and endlap) acquired from a DJI Phantom 3 Quadcopter UAV, and a 4K resolution digital camera (FC300X), an attempt has been made in this research to investigate the impact of camera calibration on the accuracy of Digital Elevation Models (DEMs) using four (4) possible case scenarios which are: (1) Processing without calibration, (2) Processing with calibration before optimization of camera alignment, (3) Processing with calibration during optimization of camera alignment and (4) Processing with calibration after optimization of camera alignment. The images were processed using Agisoft photoscan digital photogrammetric software. Eastings, Northings and Height coordinates of ground control points were extracted from the DEM generated based on these four conditions and compared with the coordinates of the same points established using Hi-Target Differential Global Positioning System (DGPS) receivers. Using the National Standard for Spatial Data Accuracy (NSSDA), the result obtained showed that though the impact was quite trivial on the Eastings and Northings coordinates extracted from the DEMs produced under these four camera calibration conditions (each producing a horizontal accuracy of 0.003786) and more evident on the height values, DEM generated by calibrating the camera before optimization of camera alignment yielded the best accuracy (with vertical accuracy of 0.08956) when compared to the other three conditions. It is thus recommended that the operation of camera calibration be performed before the optimization of camera alignment when processing UAV acquired image data for DEM production using Agisoft photoscan digital photogrammetric software.

Keywords: Camera calibration, UAV photogrammetry, 3D Elevation Models, Camera alignment, Calibration parameters, Optimization.

## INTRODUCTION

Digital elevation models (DEMs) are vital resources for various applications such as climate impact studies, water and wildlife management, geological and hydrological modelling, geomorphology and landscape analysis, earth modelling etc. (Sulebak, 2000). They can be described as spatially geo-referenced data set,that continuously represent or depict

[1] ogbajayi@gmail.com
[2] drijnwadialor@yahoo.com
[3] anyi.onuigbo@futminna.edu.ng
[4] kemiki@futminna.edu.ng

the topography of an area effectively by elevation values and snap shot of land scape features (Isioye and Paul, 2011). They can be produced from aerial photographs (Toz and Erdogan, 2008) and satellite images (Bolstad and Stowe, 1994), etc.

With the gradual influx of technology in virtually all facets of human endeavours, photogrammetry has become more globally developed, migrating from the old age-long analogue method of data acquisition and processing to digital and computerised form. The Unmanned Aerial Vehicle (UAV) has greatly thrived on the wings of technology, providing a high scale, time-effective and low-cost facility for earth monitoring (Fonstad et al., 2013; Sammartano and Spanò, 2016). Its application is fast gaining wide and public acceptance in almost all fields of human endeavours, most especially in physical sciences (Ajayi et al., 2017), and when related more specifically to photogrammetry, it has led to photogrammetry (Birute et al., 2014).

Camera calibration is one of the major steps involved in the photogrammetric processing of overlapping images for the production of DEMs (Weng et al., 1992). It is the process of finding the internal characteristics of an auto camera and finding the camera's location in space with respect to a fixed object. This is very essential when lens distortion is to be corrected or the size of the object in world units is to be measured. Cameras can be calibrated beforehand, after the flight (Anuar, 2011) or through the flight mission (Eisenbeiss, 2009) in order to extract metric information from the 2D images (Zhang, 2004), correct for lens distortion, measure the size of an object in world units, or determine the location of the camera in the scene. Norhadija et al. (2013) also opined that camera calibration is expedient if accurate and reliable measurements or results must be obtained when using UAV for environmental or photogrammetric applications.

Many calibration methods have been developed in the last couple of years (Zhang et al., 2010; Douskos et al., 2007) but most of these methods do not experiment with UAV acquired images (Pérez et al., 2011). Ahmad et al. (2017), presented the result of investigating the accuracy of camera calibration at various UAV flying heights using a Sony NEX6 digital camera, 1.5m camera distance in the laboratory, 15m and 25m camera distances on the field with the most accurate camera parameters obtained from the 25m flying height which is also the optimum object distance. Fryskowska et al. (2016) experimented Image Master Calib, MATLAB - camera calibrator application and Agisoft Lens using Sony NEX 5 digital camera. The findings showed that Agisoft lens which automatically generates large numbers of tie points (Wierzbicki et al., 2015), based on Structure from Motion (SFM) algorithms (Westboy et al., 2012), using the Semi-Global Matching (SGM) algorithm (Hirschmüller, 2005) and Scale Invariant Feature Transform (SIFT) operator (Lowe, 2004), and also has the ability to perform self-calibration, gave optimal results together with the Image Master calib.

Thus, by extension, this research investigated the implication of not calibrating the camera, calibrating before the optimization of camera locations, calibrating during the optimization of camera locations and calibrating after the optimization of camera locations during the photogrammetric processing of UAV acquired images for DEM generation.

The imaging (study) area

The imaging area is part of the main campus of the Federal University of Technology (FUT), situated in Minna, Niger state, Nigeria. Geographically, the area lies between the boundaries of Northings 1055093.867mN and 1054587.539mN, and Eastings 217981.805mE and 220613.904mE. It can be better described as a stretch from the University's Computer Based Test Center to the School of Agriculture and Agricultural Technology (SAAT) complex, encompassing the School of Environmental Technology (SET) and the University's convocation square (see Figure 1), covering an approximate area of 11 hectares. The terrain configuration is relatively gentle and flat.

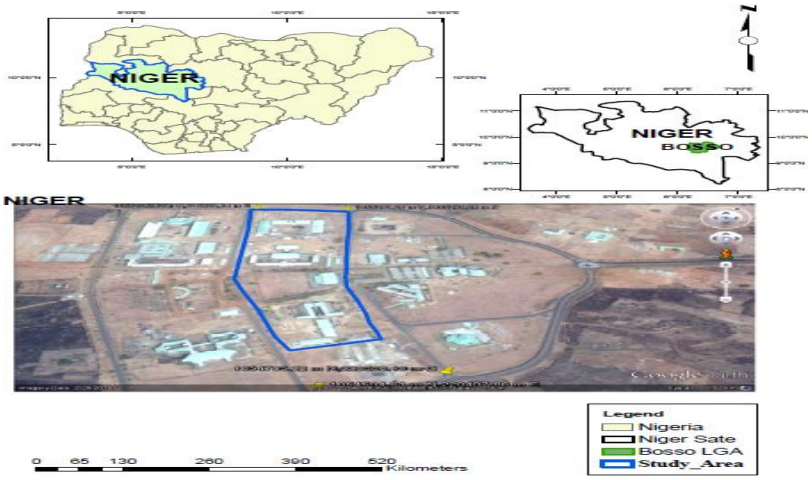


*Figure 1: Map of the imaging area.*

# METHODOLOGY

The methodology adopted is subdivided into three major components viz: reconnaissance and flight planning, image data acquisition and image processing for DEM generation. During the reconnaissance, four ground control points (GCPs) were discovered to have been previously established within the study area (GPS3, GPS6, GPS7 and GPS 12) with the aid of a High-target DGPS receiver unit. Insitu test was conducted on these GCPs and they were found to be in true position. Since these four GCPs are not sufficient, thirteen (13) more control points were also established using the same DGPS receivers, bringing the total number of GCPs to seventeen (17). The GCPs were pre-marked with reflective materials for easy identification before the flight mission. These control points were established for georeferencing, optimization of camera locations and assessment and validation of the DEMs' accuracy. DJI Phantom 3 professional; a rotary wing quadcopter UAV (see Figure 2 and Table 1 for its characteristics) was used for the image data acquisition in manual flight mode. The UAV was equipped with 12 megapixels, focal length of 2.8mm, and 4K resolution DJI FC300X camera. The camera has RGB band and operates in both manual and auto mode. The Quadcopter is powered by four (4) powerful brushless motors, with the arm span of 0.5m and weighs approximately 1.25kg including a payload of 0.75kg. To ensure a smooth and a safe flight mission, a pre-flight test was carried out to ascertain that every part of the UAV system functions properly and also, a flight plan (see figure 3) was designed to ensure total coverage of the entire imaging area and at the desired percentage overlap.


*Figure 2: DJI Phantom 3 Professional Quadcopter UAV used for the study.*

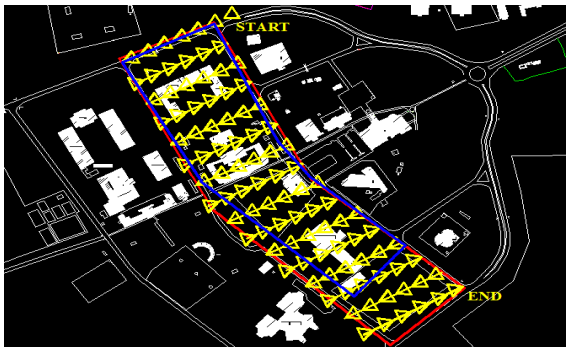


*Figure 3: Flight map showing flight lines and direction of flight of the flight mission.*

*Table 1: The characteristics of the used UAV*

| AIRCRAFT | Specifications |
|---|---|
| Weight (including battery and propellers) | 1280g |
| Diagonal size (Excluding propellers) | 350mm |
| Max Ascent Speed | 5m/s |
| Max Descent Speed | 3m/s |
| Max Speed | 16m/s (ATTI mode, no wind) |
| GPS Mode | GPS/GLONASS |
| Max Flight Time | Approximately 23 minutes |
| CAMERA | |
| Sensor | Sony EXMOR 1/2.3" Effective pixels: 12.4 M (total pixels: 12.76 M) |
| Lens | FOV 94° 20 mm f/2.8, focus at ∞ |
| Photo | JPEG, DNG |
| GIMBAL | |
| Controllable Range | Pitch -90° to +30° |
| Stabilization | 3-axis (pitch, roll, yaw) |

*(Source: http:www.dji.com/phantom3pro).*

A total of 92 images were captured in manual mode at 15-20% overlap (sidelap and endlap), and these images were all utilized for the image processing. 15-20% overlap was adopted since the imaging area is relatively small and gentle, and also, a fixed flying height was adopted. Each of the images cover an approximate area of 4004.96m$^2$. The image processing procedure involved camera calibration, optimization of camera alignment, point cloud generation, dense cloud generation, auto-mosaicking and DSM/DEM generation, all performed using the Agisoft PhotoScan software. Figure 4 describes the process flow chart for generating the DEM, while the camera calibration parameters are presented in Table 2. These parameters include the computed principal distance or focal length *(f)* of the lens, parameters *(xp, yp,)* which denote the coordinates of the center of projection of the image (principal point), and lens distortion coefficients *(k1, k2, k3, p1, p2)* where the terms *ki* represent coefficients of radial lens distortion and *pi* terms represent coefficients of decentering distortion (Perez et al., 2011) caused by a lack of centering of lens elements. Radial and decentering distortions comprise the aberrations which affect the location of images (Fryer, 1996).

*Table 2: Camera calibration parameters.*

| FC300X | | | |
|---|---|---|---|
| Resolution: 4000 x 2250 | Focal Length: 2.8 mm | Pixel Size: 4e+06 x 2.25e+06 um | Precalibrated: No |
| Type: | Frame | Skew: | -0.53316 |
| Fx: | 2305.57 | Cx: | 1995.46 |
| Fy: | 2302.89 | Cy: | 1123.9 |
| K1: | -0.130998 | P1: | -0.00043097 |
| K2: | 0.107868 | P2: | -0.000115319 |
| K3: | -0.0157875 | P3: | 0 |

| | | | |
|---|---|---|---|
| K4: | 0 | P4: | 0 |

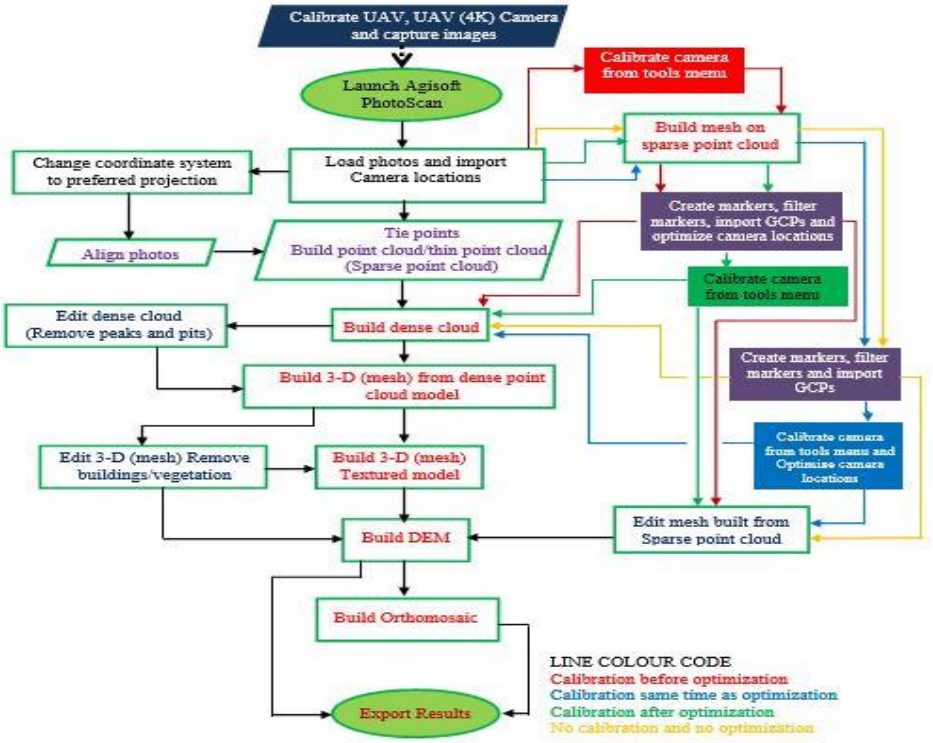


*Figure 4: Step by step process adopted for the DEM generation using different camera calibration scenarios.*

## RESULTS AND DISCUSSION OF RESULTS

Figure 5 is a pictorial representation of the location of the GCPs carefully densified across the study area while Figure 6 presents the camera locations and the error estimates. The DEM produced in case scenario (1) is presented in Figure 7. The DEM shows that the highest point in the study area has an elevation value of 267m while the height value of the lowest point is 230m. Figure 8 depicts the DEM generated in case scenario (2). The model shows that the lowest height and highest height on the imaged area is 229m and 263m respectively. The DEM produced in case scenario (3) shows that the study area has a lowest height and highest height of 229m and 263m respectively as shown in figure 9, while figure 10 presents the DEM produced in case scenario (4). It shows that the imaged area has a lowest height and highest height of 229m and 262m respectively. In order to ascertain the accuracy of each of the generated DEMs, northings, eastings and height coordinates of the ground control points earlier established were extracted from each of the DEMs. The values of these extracted coordinates were compared with the coordinate values of the same points acquired during the control establishment (GCPs). The discrepancy was computed and used for the computation of the horizontal and vertical accuracy. Table 3 contains the result obtained from case scenario (1), Table 4 contains the result obtained from case scenario (2). The result obtained from case scenarios (3) and (4) are presented in Tables 5 and 6 respectively while Table 7 contains the summary of the horizontal and vertical accuracies obtained for the four different case scenarios.

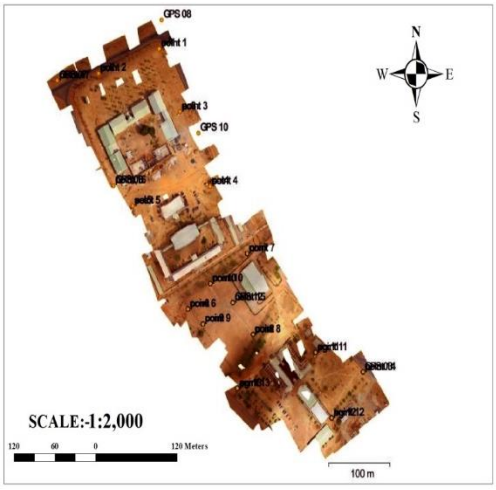


*Figure 5: Location of GCPs on the imaging (study) area.*

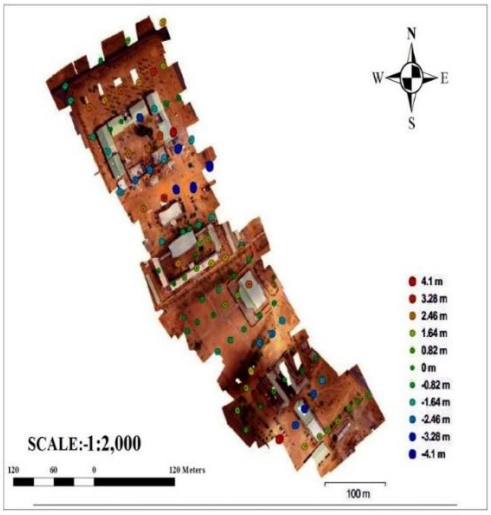


*Figure 6: Camera locations and error estimates.*

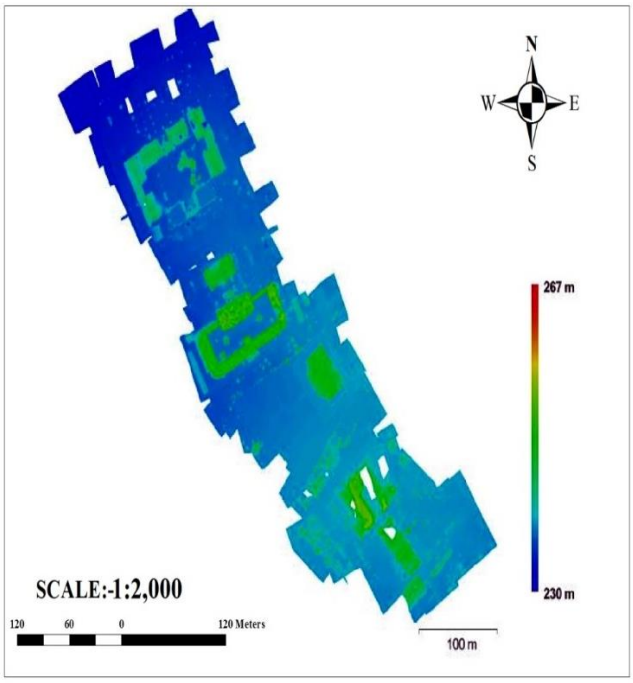


*Figure 7: DEM produced without camera calibration and before optimization of camera alignment*

.

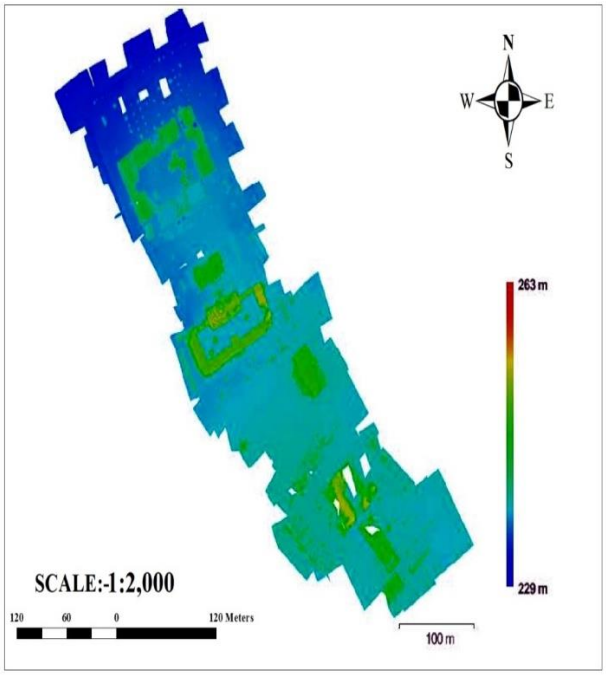


*Figure 8: DEM generated by calibrating the camera optimization of camera alignment*.

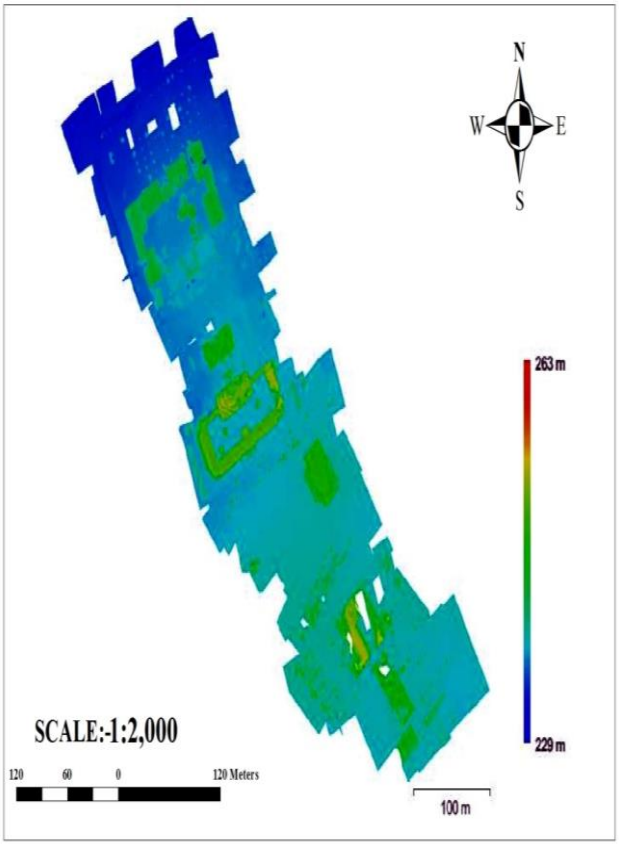


*Figure 9: DEM generated by calibrating the camera during optimization of camera alignment.*

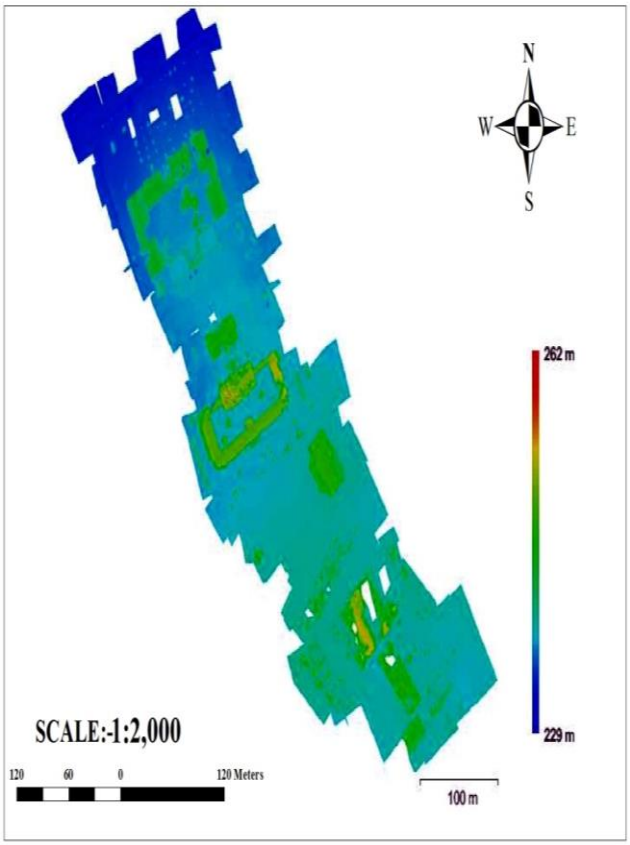


*10: DEM generated by calibrating the camera after optimization of camera alignment.*

*Table 3: Result obtained from DEM processed without camera calibration and optimization.*

| GCPs | DGPS ACQUIRED COORDINATES | | | DEM EXTRACTED COORDINATES (PROCESSING WITH NO CALIBRATION AND NO OPTIMIZATION) | | | COMPUTED DIFFERENCES | | |
|---|---|---|---|---|---|---|---|---|---|
| | E (m) | N (m) | H (m) | N (m) | E (m) | H (m) | ΔE (m) | ΔN (m) | ΔH (m) |
| PT1 | 220147.938 | 1055132.392 | 233.390 | 220149.271 | 1055131.338 | 234.575 | -1.333 | 1.054 | -1.185 |
| PT2 | 220048.540 | 1055099.532 | 232.729 | 220050.103 | 1055098.187 | 232.652 | -1.563 | 1.345 | 0.077 |
| PT3 | 220181.813 | 1055047.861 | 236.146 | 220183.007 | 1055046.715 | 236.542 | -1.195 | 1.146 | -0.396 |
| PT4 | 220230.519 | 1054946.114 | 237.100 | 220232.181 | 1054945.658 | 237.363 | -1.662 | 0.456 | -0.263 |
| PT5 | 220104.176 | 1054920.376 | 236.357 | 220105.935 | 1054919.438 | 235.874 | -1.759 | 0.938 | 0.483 |
| PT6 | 220194.365 | 1054780.450 | 237.455 | 220196.442 | 1054779.801 | 236.869 | -2.078 | 0.649 | 0.586 |
| PT7 | 220291.062 | 1054855.215 | 237.790 | 220292.918 | 1054854.724 | 237.978 | -1.856 | 0.491 | -0.188 |
| PT8 | 220300.149 | 1054745.919 | 238.512 | 220302.442 | 1054745.493 | 238.268 | -2.293 | 0.426 | 0.244 |
| PT9 | 220218.684 | 1054759.701 | 237.919 | 220220.748 | 1054759.550 | 237.351 | -2.064 | 0.151 | 0.568 |
| PT10 | 220230.353 | 1054814.547 | 237.387 | 220232.794 | 1054814.063 | 237.080 | -2.441 | 0.484 | 0.307 |
| PT11 | 220402.310 | 1054721.078 | 238.324 | 220404.502 | 1054721.238 | 238.408 | -2.192 | -0.16 | -0.084 |
| PT12 | 220427.333 | 1054633.069 | 238.563 | 220430.871 | 1054632.610 | 238.468 | -3.538 | 0.459 | 0.095 |
| PT13 | 220274.221 | 1054673.378 | 238.876 | 220276.910 | 1054672.761 | 238.472 | -2.689 | 0.617 | 0.404 |
| GPS 03 | 220479.550 | 1054694.690 | 238.015 | 220481.978 | 1054694.835 | 238.080 | -2.428 | -0.15 | -0.065 |
| GPS 06 | 220072.920 | 1054947.700 | 235.968 | 220074.561 | 1054946.622 | 235.074 | -1.641 | 1.078 | 0.894 |
| GPS 07 | 219981.297 | 1055090.510 | 231.988 | 219982.847 | 1055088.865 | 231.471 | -1.55 | 1.645 | 0.517 |
| GPS 12 | 220267.286 | 1054789.050 | 238.188 | 220269.502 | 1054788.464 | 237.798 | -2.216 | 0.586 | 0.39 |
| SUM | | | | | | | -34.500 | 11.22 | 2.383 |

*Table 4: Result obtained from DEM processed with calibration before optimization of camera alignment.*

| GCPs | DGPS ACQUIRED COORDINATES | | | DEM EXTRACTED COORDINATES (PROCESSING WITH CAMERA CALIBRATION BEFORE OPTIMIZATION OF CAMERA ALIGNMENT) | | | COMPUTED DIFFERENCES | | |
|---|---|---|---|---|---|---|---|---|---|
| | E (m) | N (m) | H (m) | E (m) | N (m) | H (m) | ΔE (m) | ΔN (m) | ΔH (m) |
| PT1 | 220147.938 | 1055132.392 | 233.390 | 220147.943 | 1055132.413 | 233.857 | -0.005 | -0.02 | -0.467 |
| PT2 | 220048.540 | 1055099.532 | 232.729 | 220048.585 | 1055099.531 | 232.696 | -0.045 | 1E-03 | 0.033 |
| PT3 | 220181.813 | 1055047.861 | 236.146 | 220181.798 | 1055047.832 | 236.172 | 0.0145 | 0.029 | -0.026 |
| PT4 | 220230.519 | 1054946.114 | 237.100 | 220230.543 | 1054946.124 | 237.172 | -0.024 | -0.01 | -0.072 |
| PT5 | 220104.176 | 1054920.376 | 236.357 | 220104.163 | 1054920.410 | 236.415 | 0.013 | -0.03 | -0.058 |
| PT6 | 220194.365 | 1054780.450 | 237.455 | 220194.215 | 1054780.288 | 237.47 | 0.1495 | 0.162 | -0.015 |
| PT7 | 220291.062 | 1054855.215 | 237.790 | 220290.986 | 1054855.225 | 237.763 | 0.0759 | -0.01 | 0.027 |
| PT8 | 220300.149 | 1054745.919 | 238.512 | 220300.182 | 1054745.948 | 238.471 | -0.033 | -0.03 | 0.041 |
| PT9 | 220218.684 | 1054759.701 | 237.919 | 220218.592 | 1054759.963 | 237.856 | 0.0922 | -0.26 | 0.063 |
| PT10 | 220230.353 | 1054814.547 | 237.387 | 220230.624 | 1054814.565 | 237.377 | -0.271 | -0.02 | 0.01 |
| PT11 | 220402.310 | 1054721.078 | 238.324 | 220402.235 | 1054721.158 | 238.306 | 0.0749 | -0.08 | 0.018 |
| PT12 | 220427.333 | 1054633.069 | 238.563 | 220427.425 | 1054632.989 | 238.547 | -0.092 | 0.08 | 0.016 |
| PT13 | 220274.221 | 1054673.378 | 238.876 | 220274.286 | 1054673.377 | 239.242 | -0.065 | 1E-03 | -0.366 |

| | | | | | | | | | |
|---|---|---|---|---|---|---|---|---|---|
| GPS 03 | 220479.550 | 1054694.690 | 238.015 | 220479.473 | 1054694.658 | 237.848 | 0.077 | 0.032 | 0.167 |
| GPS 06 | 220072.920 | 1054947.700 | 235.968 | 220072.870 | 1054947.670 | 235.671 | 0.05 | 0.03 | 0.297 |
| GPS 07 | 219981.297 | 1055090.510 | 231.988 | 219981.280 | 1055090.494 | 231.921 | 0.0174 | 0.016 | 0.067 |
| GPS 12 | 220267.286 | 1054789.050 | 238.188 | 220267.314 | 1054788.946 | 238.11 | -0.028 | 0.104 | 0.078 |
| SUM | | | | | | | 0.0006 | -0.01 | -0.188 |

*Table 5: Result obtained from DEM processed with calibration during optimization of camera alignment.*

| GCPs | DGPS ACQUIRED COORDINATES | | | DEM EXTRACTED COORDINATES (PROCESSING WITH CAMERA CALIBRATION DURING OPTIMIZATION) | | | COMPUTED DIFFERENCES | | |
|---|---|---|---|---|---|---|---|---|---|
| | E (m) | N (m) | H(m) | E (m) | N (m) | H (m) | ΔE (m) | ΔN (m) | ΔH (m) |
| PT1 | 220147.938 | 1055132.392 | 233.390 | 220147.943 | 1055132.413 | 233.900 | -0.005 | -0.021 | -0.51 |
| PT2 | 220048.540 | 1055099.532 | 232.729 | 220048.585 | 1055099.531 | 232.673 | -0.045 | 0.001 | 0.056 |
| PT3 | 220181.813 | 1055047.861 | 236.146 | 220181.798 | 1055047.832 | 236.199 | 0.0145 | 0.029 | -0.053 |
| PT4 | 220230.519 | 1054946.114 | 237.100 | 220230.543 | 1054946.124 | 237.240 | -0.024 | -0.01 | -0.14 |
| PT5 | 220104.176 | 1054920.376 | 236.357 | 220104.163 | 1054920.410 | 236.527 | 0.013 | -0.034 | -0.17 |
| PT6 | 220194.365 | 1054780.450 | 237.455 | 220194.215 | 1054780.288 | 237.439 | 0.1495 | 0.162 | 0.016 |
| PT7 | 220291.062 | 1054855.215 | 237.790 | 220290.986 | 1054855.225 | 237.515 | 0.0759 | -0.01 | 0.275 |
| PT8 | 220300.149 | 1054745.919 | 238.512 | 220300.182 | 1054745.948 | 238.527 | -0.033 | -0.029 | -0.015 |
| PT9 | 220218.684 | 1054759.701 | 237.919 | 220218.592 | 1054759.963 | 237.893 | 0.0922 | -0.262 | 0.026 |
| PT10 | 220230.353 | 1054814.547 | 237.387 | 220230.624 | 1054814.565 | 237.328 | -0.271 | -0.018 | 0.059 |
| PT11 | 220402.310 | 1054721.078 | 238.324 | 220402.235 | 1054721.158 | 238.301 | 0.0749 | -0.08 | 0.023 |
| PT12 | 220427.333 | 1054633.069 | 238.563 | 220427.425 | 1054632.989 | 238.287 | -0.092 | 0.08 | 0.276 |
| PT13 | 220274.221 | 1054673.378 | 238.876 | 220274.286 | 1054673.377 | 238.886 | -0.065 | 0.001 | -0.01 |
| GPS 03 | 220479.550 | 1054694.690 | 238.015 | 220479.473 | 1054694.658 | 237.822 | 0.077 | 0.032 | 0.193 |
| GPS 06 | 220072.920 | 1054947.700 | 235.968 | 220072.870 | 1054947.670 | 235.757 | 0.05 | 0.03 | 0.211 |
| GPS 07 | 219981.297 | 1055090.510 | 231.988 | 219981.280 | 1055090.494 | 231.950 | 0.0174 | 0.016 | 0.038 |
| GPS 12 | 220267.286 | 1054789.050 | 238.188 | 220267.314 | 1054788.946 | 238.100 | -0.028 | 0.104 | 0.088 |
| SUM | | | | | | | 0.0006 | -0.009 | 0.362 |

*Table 6: Result obtained from DEM processed with calibration after optimization of camera alignment.*

| GCPs | DGPS ACQUIRED COORDINATES | | | DEM EXTRACTED COORDINATES (PROCESSING WITH CAMERA CALIBRATION AFTER OPTIMIZATION) | | | COMPUTED DIFFERENCES | | |
|---|---|---|---|---|---|---|---|---|---|
| | E (m) | N (m) | H(m) | E (m) | N (m) | H (m) | ΔE (m) | ΔN (m) | ΔH (m) |
| PT1 | 220147.938 | 1055132.392 | 233.390 | 220147.943 | 1055132.413 | 233.948 | -0.0051 | -0.021 | -0.558 |
| PT2 | 220048.540 | 1055099.532 | 232.729 | 220048.585 | 1055099.531 | 232.684 | -0.0447 | 0.001 | 0.0453 |
| PT3 | 220181.813 | 1055047.861 | 236.146 | 220181.798 | 1055047.832 | 236.164 | 0.0145 | 0.029 | -0.018 |
| PT4 | 220230.519 | 1054946.114 | 237.100 | 220230.543 | 1054946.124 | 237.195 | -0.0242 | -0.01 | -0.0954 |
| PT5 | 220104.176 | 1054920.376 | 236.357 | 220104.163 | 1054920.410 | 236.560 | 0.013 | -0.034 | -0.2034 |
| PT6 | 220194.365 | 1054780.450 | 237.455 | 220194.215 | 1054780.288 | 237.415 | 0.1495 | 0.162 | 0.0402 |
| PT7 | 220291.062 | 1054855.215 | 237.790 | 220290.986 | 1054855.225 | 237.559 | 0.0759 | -0.01 | 0.2308 |
| PT8 | 220300.149 | 1054745.919 | 238.512 | 220300.182 | 1054745.948 | 238.520 | -0.0333 | -0.029 | -0.0082 |

| | | | | | | | | | |
|---|---|---|---|---|---|---|---|---|---|
| PT9 | 220218.684 | 1054759.701 | 237.919 | 220218.592 | 1054759.963 | 237.906 | 0.0922 | -0.262 | 0.0134 |
| PT10 | 220230.353 | 1054814.547 | 237.387 | 220230.624 | 1054814.565 | 237.399 | -0.2713 | -0.018 | -0.0122 |
| PT11 | 220402.310 | 1054721.078 | 238.324 | 220402.235 | 1054721.158 | 238.306 | 0.0749 | -0.08 | 0.0176 |
| PT12 | 220427.333 | 1054633.069 | 238.563 | 220427.425 | 1054632.989 | 238.293 | -0.0924 | 0.08 | 0.2696 |
| PT13 | 220274.221 | 1054673.378 | 238.876 | 220274.286 | 1054673.377 | 238.856 | -0.0647 | 0.001 | 0.0201 |
| GPS 03 | 220479.550 | 1054694.690 | 238.015 | 220479.473 | 1054694.658 | 237.794 | 0.077 | 0.032 | 0.221 |
| GPS 06 | 220072.920 | 1054947.700 | 235.968 | 220072.870 | 1054947.670 | 235.453 | 0.05 | 0.03 | 0.5146 |
| GPS 07 | 219981.297 | 1055090.510 | 231.988 | 219981.280 | 1055090.494 | 231.953 | 0.0174 | 0.016 | 0.0354 |
| GPS 12 | 220267.286 | 1054789.050 | 238.188 | 220267.314 | 1054788.946 | 238.108 | -0.0281 | 0.104 | 0.0798 |
| SUM | | | | | | | 0.0006 | -0.009 | 0.5926 |

*Table 7: Analysis of the RMSE, horizontal and vertical accuracies obtained for the four different case scenarios.*

| S/N | CONDITIONS | RMSEr | RMSEz | HORIZONTAL ACCURACY | VERTICAL ACCURACY |
|---|---|---|---|---|---|
| 1 | No camera calibration | 8.79825854 | 0.57786538 | 15.22802588 | 1.132616145 |
| 2 | Calibration before optimization of camera Alignment | 0.002187666 | 0.045693712 | 0.003786412 | 0.089559675 |
| 3 | Calibration during optimization of camera alignment | 0.002187666 | 0.087700882 | 0.003786412 | 0.171893729 |
| 4 | Calibration after optimization of camera alignment | 0.002187666 | 0.143726611 | 0.003786412 | 0.281704158 |

The Root Mean Square Error (RMSE) was calculated using the formula given in equation (1):

$$RMSE = \sqrt{\frac{\sum(N_i - N_j)^2}{n}} \quad (1)$$

Where $N_i$ is observed values, $N_j$ is reference values and $n$ is number of points.

The horizontal and vertical accuracy was computed using the National Standard for Spatial Data Accuracy (NSSDA) method for map accuracy which is given as equations (2) and (3):

$$\text{Horizontal Accuracy} = 1.7308 \times \text{RMSE}_r \quad (2)$$

$$\text{Vertical Accuracy} = 1.96 \times \text{RMSE}_Z \quad (3)$$

Where $\text{RMSE}_r$ and $\text{RMSE}_Z$ are the Root mean square errors of the horizontal and vertical discrepancy respectively.

From the results obtained, it was discovered that case scenario (1) gave coordinate values that are of widest variance when compared with the coordinate values of DPGS observation. Change in Eastings (ΔE) of -34.500m, Changes in Northings (ΔN) of 11.22m and Height (ΔH) of 2.383m were observed and recorded, while case scenario (2) gave the lowest discrepancy value with ΔE of 0.0006m, ΔN of -0.01m and ΔH of -0.188m. Case scenarios (3) and (4) gave ΔE and ΔN values of 0.0006m and -0.009m respectively with a ΔH value of 0.362m for case scenario (3) and ΔH value of 0.5926m for case scenario (4). Also, a horizontal accuracy of 15.228 and vertical accuracy of 1.133 was obtained from the analysis of case scenario (1), horizontal accuracy of 0.003 was obtained from case scenarios (2), (3) and (4) respectively (see Table 7). This implies that the timing of camera calibration (before during or after the optimization of camera alignment) has no implication on the horizontal accuracy of the generated DEMs. Vertical accuracy of 0.089 was obtained from case scenario (2), while 0.171 was obtained from case scenario (3) and 0.281 obtained from case scenario (4). This shows that the timing of camera calibration (before, during or after the optimization of camera alignment) has a great impact on the obtainable vertical accuracy of DEMs even though the horizontal reliability of the generated DEM seems immune to this. From our results, the vertical accuracy obtained from case scenario (2) where the camera was calibrated before the optimization of camera alignment

was the lowest (closest to zero) and thus, most accurate of the four different case scenarios. This was closely followed by case scenario (3) and then case scenario (4).

## CONCLUSIONS

It was discovered from the obtained results that the coordinates extracted from the DEM generated via a process where the camera was calibrated before the optimization of camera alignment were closer to the coordinates obtained from the field observation using High-target DGPS receivers when compared to the other three case scenarios. This method gave a horizontal accuracy of 0.003 and a vertical accuracy of 0.089. It is thus necessary to ensure that the operation of camera calibration is performed before the optimization of camera alignment when processing image data of this nature for DEM production using the Agisoft photoscan digital photogrammetric software. Also, it was discovered that the same horizontal accuracy was obtained from the processes where the camera was calibrated before, during and after the optimization of camera alignment which means that the timing of camera calibration has little or no effect on the horizontal or planimetric integrity of the produced DEMs. Finally, the worst (most inaccurate) result was obtained from case scenario (1) which means that camera calibration is highly important in the production of DEMs from UAV acquired overlapping images.

## ACKNOWLEDGEMENT

The authors would like to thank Messers Salubi Anthony, Angbas Fred and Godfrey Mukwedeh for their kind assistance during the image data acquisition and processing stages of this research.

## REFERENCES

Ahmad, R. Y., Mohd, F. M. A., Khairulnizam, M. I., Zulkepli, M., and Albert, K. C. (2017) Camera Calibration Accuracy at different UAV Flying Heights. The International Archives of the Photogrammetry, Remote Sensing and Spatial Information Sciences, Volume XLII-2/W3, 2017 3D Virtual Reconstruction and Visualization of Complex Architectures, 1–3 March 2017, Nafplio, Greece, pp. 595-600

Ajayi, O. G., Salubi, A. A., Angbas, A. F., and Odigure, M. G. (2017) Generation of accurate digital elevation models from UAV acquired low percentage overlapping images. International Journal of Remote Sensing. 8-10(38), pp. 3113-3134.

Anuar, A. (2011) Digital Mapping Using Low Altitude UAV. Pertanika Journal of Science and Technology. 19 (S), pp. 51-58.

Birute, R., Tautvydas, B., Silvija, G., Edita, J., and Vladislovas C. A. (2014) Photogrammetric Processing of UAV Imagery: Checking DTM. The 9th International Conference "Environmental Engineering" 22–23 May 2014, Vilnius, Lithuania. Available online at http://enviro.vgtu.lt

Bolstad, P. V. and Stowe, T. (1994) An Evaluation of DEM Accuracy: Elevation, Slope and Aspect, Photogrammetric Engineering and Remote Sensing. 60(11), pp. 1327-1332.

Douskos V., Kalisperakis I. and Karras G. 2007. Automatic calibration of digital cameras using planar chessboard patterns. 8th Conf. Opt. 3-D Meas. Techn., Wichmann, vol. I, pp. 132-140.

Eisenbeiss, H., (2009). UAV Photogrammetry, PhD Thesis, University of Technology Dresden, Zurich, Germany.

Fonstad, M.A., Dietrich, J.T., Courville, B.C., Jensen, J.L. and Carbonneau, P.E. (2013) Topographic structure from motion: a new development in photogrammetric measurement. Earth Surf. Process. Landforms. 38, pp. 421–430.

Fryer, J.G. (1996) Camera calibration. In: Close Range Photogrammetry and Machine Vision. K.B. Atkinson (Eds), Whittler Publishing, Caithness, pp. 156-179.

Fryskowska, A., Kedzierski, M., Grochala, A., and Braula, A. (2016) Calibration of Low-Cost RGB And NIR UAV Cameras. The International Archives of the Photogrammetry, Remote Sensing and Spatial Information Sciences, Volume XLI-B1, 2016 XXIII ISPRS Congress, 12–19 July 2016, Prague, Czech Republic, pp. 817-821.

Hirschmüller, H. (2005) Accurate and Efficient Stereo Processing by Semi-Global Matching and Mutual Information, IEEE Conference on Computer Vision and Pattern Recognition, June 2005, San Diego, CA, USA, Volume 2, pp. 807-814.

Isioye, O. A and Jobin, P. (2011) An Assessment of Digital Elevation Models (DEMs) From Different Spatial Data Sources. In Proceedings of the FIG Working Week 2011, Bridging the Gap between Cultures Marrakech, Morocco, 18-22 May 2011.

Lowe, D. (2004) Distinctive Image Features from Scale-Invariant Keypoints. International Journal of Computer Vision, 60(2), pp. 91-110.

Norhadija, D., Nurul, F.A.H., Wani, S.U., Noor, A.B.M.A., and Anuar, A. (2013) Light Weight Rotary-Wing UAV for Large Scale Mapping Applications. Asia Geospatial Forum, 24-26 September 2013, Kuala Lumpur, Malaysia.

Pérez, M., Agüera, F., and Carvajal, F. (2011) Digital camera calibration using images taken from an unmanned aerial vehicle. International Archives of the Photogrammetry, Remote Sensing and Spatial Information Sciences, Vol. XXXVIII-1/C22 UAV-g 2011, Conference on Unmanned Aerial Vehicle in Geomatics, Zurich, Switzerland, pp. 1-5

Sammartano, G. and Spanò, A. (2016) DEM Generation based on UAV Photogrammetry Data in Critical Areas. In Proceedings of the 2nd International Conference on Geographical Information Systems Theory, Applications and Management (GISTAM 2016), pp. 92-98

Sulebak, J. R. (2000) Applications of Digital Elevation Models. DYNAMAP " White Paper", 2000, pp.1-11

Toz, G. and Erdogan, M. (2008) DEM (digital elevation model) production and accuracy modelling of DEMs from 1:35.000 scale aerial photographs. The International Archives of the Photogrammetry, Remote Sensing and Spatial Information Sciences. Vol. XXXVII. Part B1. Beijing 2008, pp. 775-780

Weng, J., Cohen, P., and M. H. 1992. Camera calibration with distortion models and accuracy evaluation. IEEE Trans, Pattern Analysis and Machine Intelligence, vol.14, no.10, October 1992, pp. 965-980.

Westboy, M. J., Brasington, J., Glasser, N. F., Hambrey, M. J., and Reynolds, J. M. (2012) Structure-from-Motion Photogrammetry: A low-cost, effective tool for geoscience applications. Geomorphology, 179, pp. 300-314.

Wierzbicki, D., Kedzierski, M., and Fryskowska, A. (2015) Assessment of the influence of UAV image quality on the orthophoto production. The International Archives of the Photogrammetry, Remote Sensing and Spatial Information Sciences, Volume XL-1/W4, 2015.

Zhang, W., Jiang, T. and Han, M. 2010. Digital camera calibration method based on PhotoModeler. 3rd International Congress on Image and Signal Processing (CISP2010), pp. 1235-1238.

Zhang, Z. (2004) Camera Calibration. In G. Medioni and S. B. Kang (eds.), Emerging Topics in Computer Vision, Prentice Hall Professional Technical Reference, Chapter 2, 4-43.

END